

## Paratuberculosis in a Goat: A Rare Type III C (Paucibacillary) Granulomatous Ileitis with Disseminated Secondary Lesions

N. Babu Prasath<sup>1</sup>, K. P. Singh<sup>1\*</sup>, Pawan Kumar<sup>1</sup>, M. Saminathan<sup>1</sup>, R. Singh<sup>1</sup>, K. Sindhoora<sup>1</sup>, K. Abinaya<sup>2</sup>, A. T. Faslu Rahman<sup>1</sup>

<sup>1</sup>Division of Pathology, ICAR-Indian Veterinary Research Institute, Izatnagar-243122, Bareilly, Uttar Pradesh, INDIA

<sup>2</sup>Division of Microbiology, ICAR-Indian Veterinary Research Institute, Izatnagar-243122, Bareilly, Uttar Pradesh, INDIA

\*Corresponding Author: [karamcadrad62@gmail.com](mailto:karamcadrad62@gmail.com)

**How to cite this paper:** N, B., Singh, K., Kumar, P., M, S., Singh, R., & K, S. et al. (2020). Paratuberculosis In A Goat: A Rare Type III C (Paucibacillary) Granulomatous Ileitis With Disseminated Secondary Lesions. International Journal of Livestock Research, 10(9), 222-229. doi: <http://dx.doi.org/10.5455/ijlr.20200622.072519>

**Received** : Jun 22, 2020  
**Accepted** : Jul 30, 2020  
**Published** : Sep 30, 2020

Copyright © Prasath *et al.*, 2020

This work is licensed under the Creative Commons Attribution International License (CC BY 4.0). <http://creativecommons.org/licenses/by/4.0/>



### Abstract

*A five years old full-term cross bred female goat was presented for necropsy with the history of chronic weakness for six months. On external examination, carcass was emaciated and showed pale mucous membranes and soiling of perineum with pasty faeces. On detailed examination, distal small intestine (part of distal jejunum and ileum) revealed irregular, rough, multifocal areas of mucosal thickening. Scattered areas showed mucosal wrinkles. Ileocecal valve was congested and thickened. Mesenteric lymph nodes (MLNs) were enlarged and oedematous. Microscopically, ileum revealed villi distortion, atrophy and fusion. Tips of the villi were blunt and fused. Lamina propria was widened with aggregates of lymphocytes and macrophages. Epithelioid cells were clustered at the centre of the lymphoid aggregation forming a granuloma. Multinucleated giant cells were found within the granuloma. Submucosa revealed lympho-plasmacytic infiltration, oedema and fibrinous exudation. Lymphatic vasculitis with thrombus was seen at the submucosa. Disseminated granulomatous lesions were noticed in liver, lungs and kidney. Lung revealed oedema, focal granuloma and perivascular lymphocytic infiltrations. Liver showed paracentral necrosis. Acute splenitis was also noticed. Kidney revealed congestion and focal granuloma. The MLNs revealed intrafollicular granuloma with typical Langhans-type giant cells at the paracortical zone. Ziehl-Neelsen staining of intestinal scrapings and lymph node impression smear along with tissues sections from ileum revealed scattered acid-fast bacilli within and outside the macrophages. The PCR amplification of MAP IS900 gene was carried out using IS900 primers in tissues of jejunum, ileum and MLNs showed positive amplicon of 572 bp. Based on the histopathomorphological features, this case was diagnosed as multifocal paucibacillary type III subtype c paratuberculosis in a goat.*

**Keywords:** Goat, paratuberculosis, pathology, polymerase chain reaction, type III paucibacillary, ZN staining

## Introduction

Paratuberculosis or Johne's disease, (JD) is a chronic disease of ruminants caused by *Mycobacterium avium* subspecies *paratuberculosis* (MAP) (Whittington *et al.*, 2017). The MAP resides within the M cells of Peyer patches and in macrophages of small intestine and its associated lymph nodes. MAP infection results in granulomatous enteritis, a chronic inflammation of intestine. Paratuberculosis is primarily a disease of ruminants and camelids (Whittington *et al.*, 2017), but it is also reported from diverse species of animals and thought to be associated with Crohn's disease in humans (Kirkwood *et al.*, 2009). Paratuberculosis gained importance by its huge economic losses in farmed livestock due to decreased milk production, weight loss and mortality (Caspersen, 2003). JD in small ruminants is clinically characterized by progressive weight loss, soft faeces and intermittent diarrhoea (Copra *et al.*, 2000). Gross intestinal corrugations are less pronounced in small ruminants and rather histologically show very similar lesions on par with cattle, which is characterised by granulomatous enteritis and lymphadenitis. Diagnosis is challenging in small ruminants as it may occur as multibacillary or paucibacillary type (Clark, 1997; Garg *et al.*, 2015). Histopathological changes, severity of lesions and morphology of granulomatous cell population classifies paratuberculosis into three types (Perez *et al.*, 1996). This case reports the occurrence of type III subtype c, multifocal paucibacillary paratuberculosis in a goat of Bareilly, Uttar Pradesh.

## Material and Methods

A carcass of five years old cross bred female goat was presented for necropsy examination to the Division of Pathology, ICAR-Indian Veterinary Research Institute, Izatnagar, Bareilly, Uttar Pradesh with the history of chronic wasting, progressive weakness despite of good nutrition for past one year. Reported that animal had intermittent diarrhoea. Detailed necropsy examination was done as per the standard procedure.

Representative tissue samples from different organs were collected in 10% neutral buffered formalin for histopathology. Smears were made from mucosal scrapings of distal jejunum, ileum, ileocecal valve and impression smears from cut surface of mesenteric lymph nodes and fixed with methanol for Ziehl-Neelsen staining for demonstration of acid-fast organisms. Tissue samples from distal jejunum, ileum, and MLNs were collected in a sterile container for polymerase chain reaction (PCR).

Formalin fixed tissues were processed by paraffin embedding technique, 4-5  $\mu$  thick tissue sections were prepared and stained with haematoxylin and eosin (H&E) staining as per the standard histological procedure (Bancroft and Layton, 2019).

Ziehl-Neelsen staining of mucosal scrapings and parallel tissue sections from the jejunum, ileum and MLNs was done as per the standard protocol (Morris *et al.*, 2019)

PCR was used to detect MAP gene as described by Collins *et al.* (1993). DNA extracted using QIAamp DNA Mini kit (Qiagen, Germany) from jejunum, ileum and MLNs were further amplified using specific IS900 forward and reverse primers (IS900 forward primer sequence was 5'- GGG TTG ATC TGG ACA ATG ACG GTT A-3' and IS900 reverse primer sequence was 5'- AGC GCG GCA CGG CTC TTG TT-3') and Dream Taq PCR Master mix (2X). IS900 PCR amplification was performed in a thermocycler (Biometra T1 thermoblock, Germany) with following cycles as initial denaturation at 95°C for 5 min, followed by 40 cycles of denaturation and annealing at 94°C for 45 seconds and 68°C for 45 seconds respectively, elongation with 72°C for 45 seconds and final elongation at 72°C for 10 minutes. The resulting PCR amplified products were mixed with 6X gel loading dye and subjected to submarine gel electrophoresis in 1.5% agarose gel containing ethidium bromide @ 0.5  $\mu$ g/ml using 1X TAE buffer (pH 8.0) at 100V. The gel was examined in gel documentation system (BioRad Molecular Image Gel Doc TM XR+ Image system (BioRad, USA) to confirm the size of the product.

## Results and Discussion

During necropsy, on external examination, visible mucous membrane was pale. The tail and perineal regions were smeared with dark green coloured pasty faeces. On internal examination, thoracic and abdominal cavity revealed tan yellowish clear fluid of about 100 ml and 200 ml, respectively. Epicardium revealed few petechiae around the coronary groove. Both the lungs were slightly congested and showed scattered areas of consolidation. An irregular greyish white patchy necrotic area was obvious over the visceral surface of the right caudal lobe of liver. On incision,

lesion stretched deep into the parenchyma. Terminal small intestine (distal jejunum and ileum) and caecum along with part of colon were murky and showed mild serosal congestion. On opening of the lumen of intestine, mucosa of the distal jejunum and ileum was slightly congested and were irregularly thick, bumpy with wrinkles (Fig. 1). Ileocecal valve (ICV) was found to be weathered and bumpy. Mesenteric lymph nodes (MLNs) were hulky in appearance. Few of the MLNs were caricatured. Cut sections of MLNs revealed multiple pale white foci at the cortex. Uterus was distended and contained two full term male foetuses. No lesions could be observed in foetuses.

Histopathology of ileum revealed thickening of the mucosal layer which were thrown into folds (Fig. 2.). Villi exhibited changes like distortion, thickening, atrophy and fusion. Villi at the affected portions were broad and flattened/blunt at the tip, also lacteals were minuscules and vessels were congested. Lamina propria was inflated with accumulation of mononuclear cells, predominantly of lymphocytes (Fig. 2). Aggregates of lymphocytes occupies entire lamina propria extend from basal layer to villi. Macrophages and plasma cells were infiltrated into the lamina propria. Throng of epithelioid cells (Fig. 3) were seen at the centre of the aggregative lymphocytes forming a microgranuloma. Epithelioid cells were fused to form multinucleated giant cells and few resembling a typical “baby foot appearance” (Fig. 4). Submucosa was thickened with mononuclear cells (lymphocytes and plasma cells) infiltration and collagenous tissue. Submucosal oedema with eosinophilic fibrinous material was described extending from the submucosa to muscularis mucosa (Fig. 7). Lymphocytic and plasma cells infiltration was perceived and more pronounced in the submucosa, latter was characterised by oval cell contour with eosinophilic cytoplasm and nucleus selvaged towards periphery. Submucosa revealed perivascular lympho-plasmacytic infiltration (Fig. 5) and vascular organised thrombus (Fig. 6). Serosa was thick with slight fibrous tissue procreation and lymphocytic infiltration (Fig. 5).

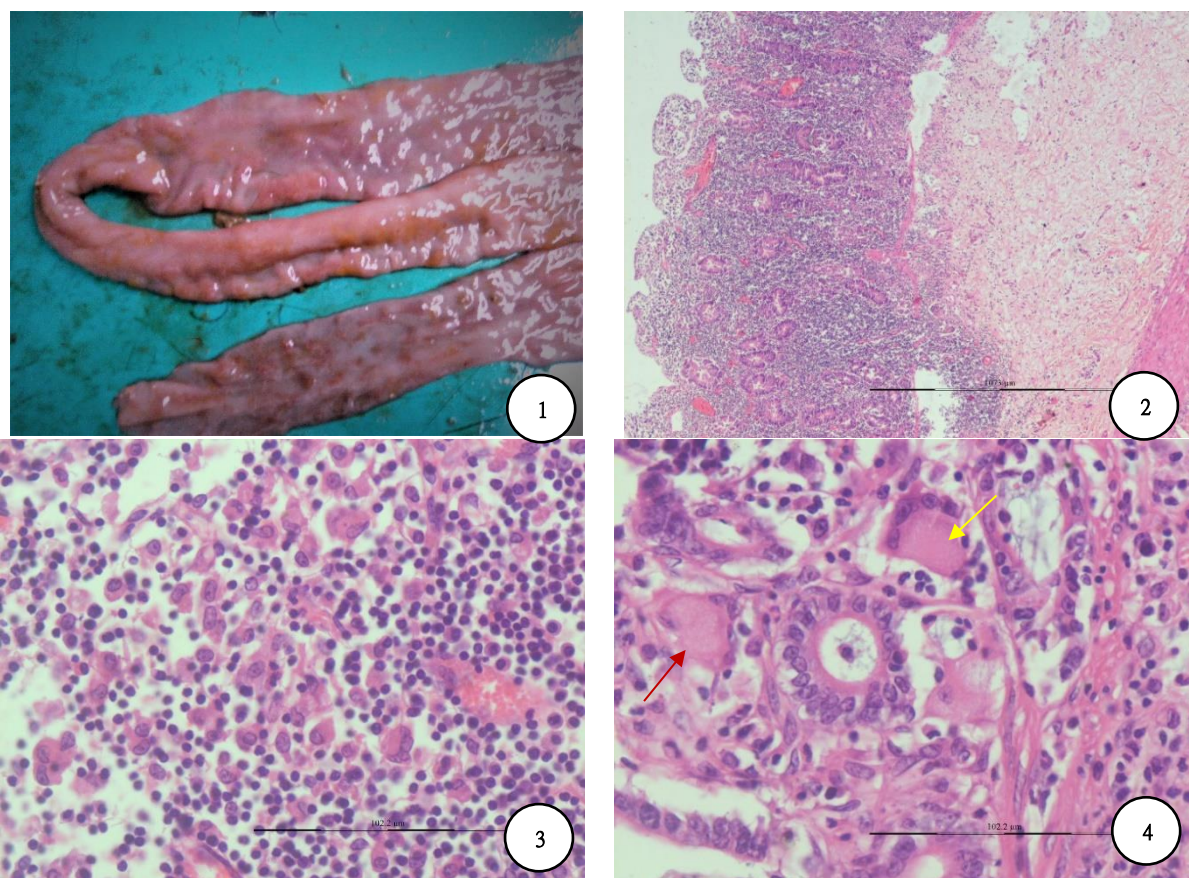


Fig. 1. Patchy irregular gross thickening and wrinkles of intestinal mucosa – Ileum. Fig. 2. Thickening and congestion of mucosa, widening of lamina propria due to lymphocytic infiltrations with distortion, fusion of villi, flattening of villus tips and submucosa of intestine –Ileum H&E x10. Fig. 3. Accumulation of macrophages, epithelioid cells and syncytial cells in lamina propria –Ileum H&E x40. Fig. 4. Multinucleated giant cells (red arrows) with typical “baby foot appearance” (yellow arrow) – Ileum H&E x40.

MLNs revealed presence of multinucleated Langhans-type giant cells (Fig. 8) at the paracortical areas accompanied by mild oedema. Aggregation of epithelioid cells and subsequent formation of microgranuloma were prominent at the centre of the lymphoid follicles. Epithelioid cells are characterised by prominent and eosinophilic cytoplasm with large euchromic round nuclei.

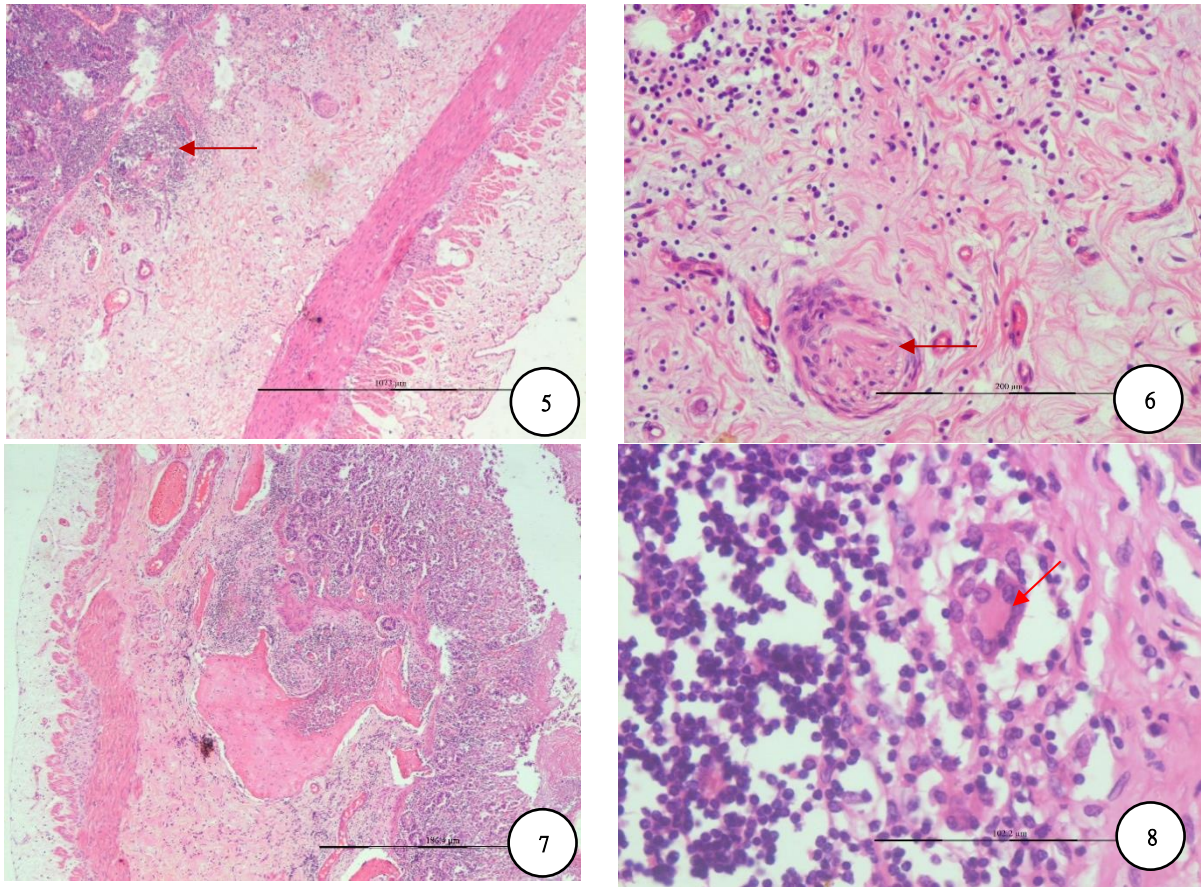


Fig. 5. Widening of submucosa, lympho-plasmacytic infiltrations, perivascular MNC aggregation (arrow), thickening of tunica serosa – Ileum H&E x10. Fig. 6. Vascular organised thrombus (arrow) with lympho-plasmacytic infiltrations of submucosa – Ileum H&E x40. Fig. 7. Submucosal oedema, MNC infiltrations with fibrinous exudate – Ileum H&E x40. Fig. 8. Langhans-type giant cell (arrows) – paracortex – Mesenteric lymph node H&E x100.

Lungs revealed severe congestion, intra-alveolar oedema and moderate thickening of alveolar septa. Lymphocytes and few neutrophils infiltrate the alveolar wall (Fig. 11). Focal granuloma was noticed. Perivascular lymphocytic infiltrations were evident near terminal bronchiole. Liver showed subcapsular and paracentral necrosis (Fig. 12) with infiltration of neutrophils and lymphocytes. Microgranuloma was evident near the periphery of necrotic parenchyma. Hepatocytes were revealed vacuolar degeneration. Spleen revealed acute splenitis with fairly high infiltration of neutrophils into the parenchyma and in trabeculae. Splenic parenchyma showed mild lymphoid depletions in white pulp and congestion. Splenic capsule was thick with moderate fibrous tissue proliferation. Kidney revealed congestion and focal granuloma.

Intestinal scrapings revealed several scattered acid-fast bacilli, within the cytoplasm of macrophages and giant cells and few were found to be outside the cells. Tissue sections of distal jejunum, ileum and MLNs revealed acid-fast bacilli scattered in the lamina propria and found within the macrophages (Fig. 9), epithelioid cells and giant cells. Bacilli were fewer rather aggregation within the cells.

Amplification of MAP IS900 gene from distal jejunum, ileum and MLNs showed 572bp amplicon size (Fig. 10).

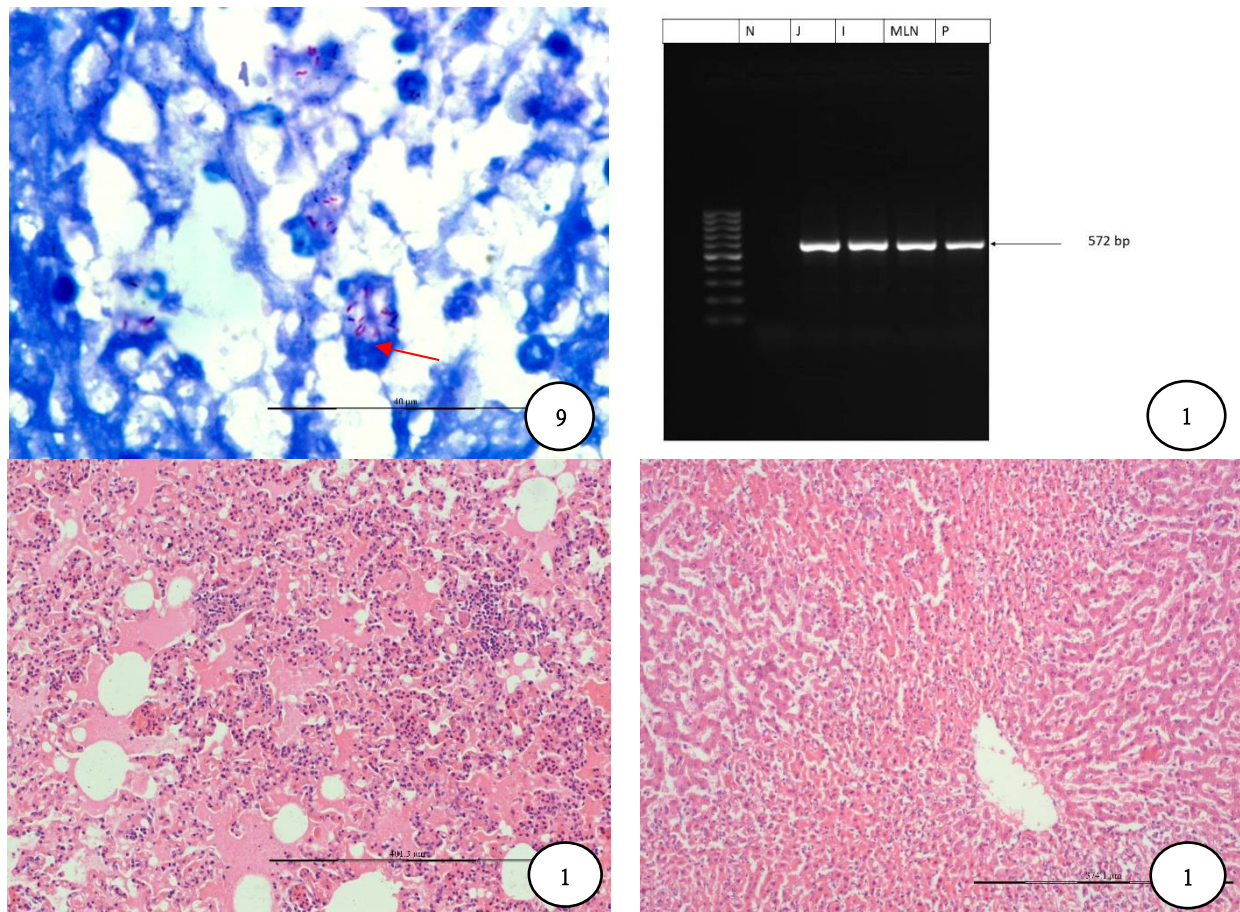


Fig. 9. Acid fast bacilli (AFB) within macrophage and epithelioid cells – ileum (Ziehl-Neelson stain) x100. Fig. 10. PCR amplification of MAP IS 900 gene with 572 amplicon products from jejunum (J), Ileum (I) and Mesenteric lymph node (MLN). Fig. 11. Lung sections showing severe pulmonary oedema, thickening of alveolar wall with infiltration of lymphocytes and neutrophils, focal granuloma H&E x20. Fig. 12. Paracentral hepatic necrosis H&E x20.

The first chronicle about paratuberculosis was reported in Germany by Johne and Frothingham (1895) and later it was named exclusively as Johne’s disease. Paratuberculosis is worldwide in distribution and highly endemic in dairy herds of developed countries including India (Singh *et al.*, 2016).

The JD is a chronic disease caused by *Mycobacterium avium* subspecies *paratuberculosis* (MAP) characterized by its long incubation period (1-14 years) (Whittington and Sergeant, 2001). Large ruminants showed higher prevalence (24.1%) than sheep and goats (22.5) (Singh *et al.*, 2016). The clinical manifestation of paratuberculosis ranges from silent, sub-clinical, clinical to advanced clinical forms (Whittington and Sergeant, 2001). Subclinical disease needs special attention for diagnosis as clinical symptoms are either less severe or entirely absent (Chiodini *et al.*, 2012). Histopathological and molecular techniques are required to confirm such subclinical disease (Garg *et al.*, 2015).

Histologically, two forms of paratuberculosis were described in small ruminants, namely multibacillary and paucibacillary (Clark, 1997). Multibacillary is characterised by granulomatous enteritis, typically dominated by macrophages filled with abundant acid-fast bacilli and affected animal tend to have strong Th-2 humoral immune response (Catton, 2002; Dennis *et al.*, 2011). Granulomatous enteritis characterised by dominated lymphocyte population with either insignificant or scarce acid-fast bacilli are classified as paucibacillary and affected animal likely to have an associated Th-1 cell-mediated immune response (Clarke, 1997). Among, the paucibacillary form occur less often and more incessant in sheep than in other brute (Copra, 2000). Reports on occurrence of paucibacillary paratuberculosis in goat were skimpy and was first portrayed by Fiorentino *et al.* (2012).

In the present case, grossly, typical corrugations were less pronounced and mostly presents as irregular thickening of intestinal mucosa are in accordance with earlier reports in small ruminates (Perez *et al.*, 1996; Vineetha *et al.*, 2018). The histological lesions such as widened intestinal villi and accumulation of mononuclear cells along with Langhans-type giant cells observed in the present study were very similar with the previous reports of paratuberculosis in goats (Rajkumar and Tripathi, 2005; Fiorentino *et al.*, 2012; Monika *et al.*, 2017, Vineetha *et al.*, 2018), sheep (Hailat *et al.*, 2010; Sikandar *et al.*, 2013), and cattle and buffalo (Sikandar *et al.*, 2012).

Perez *et al.* (1996) described paratuberculosis of small ruminants based on the severity of histopathological lesions in intestine and mesenteric lymph node into type I (mild focal), II (focal), and IIIa,b,c (multifocal, multifocal to diffuse-multibacillary and multifocal to diffuse-paucibacillary respectively) type. Type I lesion composed of granuloma with high density of macrophages. Granuloma are most commonly seen predominantly in Peyer's patches at its basal zone. No AFB (acid-fast bacilli) can be demonstrated. Gross intestinal lesions were absent. Type II lesion includes more severe form of type I, noticed in Peyer's patches and rather granuloma extend from basal zone to apex penetrating the lamina propria mucosae. Number of AFB are scanty. No gross intestinal lesions are present. Type III lesion composed of granuloma of lymphoid tissue (Peyer's patches) and non-lymphoid tissues (mucosa), which further subdivided into three subtypes: subtype *a*, characterised by granuloma of Peyer's patch and its related mucosa. Granuloma is multifocal and were seen in ileum less in jejunum. The submucosa and serosa contain scanty inflammatory cells (lymphocytes and macrophages). Number of AFB are abundant but may invariable. The only gross lesions observed are a slight enlargement of serosal lymph vessels of the ileum. Type III subtype *b* is characterised by a diffuse granulomatous enteritis (Peyer's patches and both lymphoid and non-lymphoid mucosa) formed by groups of epithelioid cells, giving a mosaic-like appearance to the mucosa. The intestinal villi were strikingly increased in thickness and their apices appeared flat and wide; the villi are rarely fused. Lymphocytes and plasma cells appeared among the epithelioid cells in small numbers. Poorly defined giant cells are present. Submucosa contain lymphocyte and plasma cell infiltrates and are located around vessel as perivascular arrangement which may extend up to the muscular layer. Lymphatic vessels were dilated and thrombi can be seen within them. Lymphangitis and lymphangiectasis in different degrees are present in serosa. Both mesenteric and ileocecal lymph nodes show a diffuse or multifocal granulomatous lymphadenitis. Number of AFB are always abundant. Grossly, intestinal wall become thickened and mucosa show corrugations particularly in ileum and occasionally jejunum. Serosal lymphatics become thickened as cords. Mesenteric and ileocecal lymph nodes become enlarged and edematous. Necrosis and calcification are absent. Type III subtype *c* is characterised by diffuse granulomatous enteritis similar but severe than subtype-*b*. Granuloma is composed of pyknotic macrophages and giant cells. Predominant inflammatory cells are lymphocytes infiltrating the entire lamina propria of both the villi and the basal area. Plasma cells and well-differentiated giant cells are seen. Submucosal oedema is frequent, together with a variable number of lymphocytes and plasma cells arranged in groups. Granuloma in lymph nodes are present in paracortical and intrafollicular areas. The main pathological feature is the presence of Langhans-type giant cells in lymph nodes. AFB is absent or scanty if present. Grossly, intestinal thickening is obvious with no areas of caseation and calcification. Typical corrugations of type III subtype *b* are absent (Perez *et al.*, 1996).

Based on the coincidence of microscopic observations such as mucosal lymphocytic aggregations with demonstration of scarce acid-fast positive organisms of the present study with the earlier observation of paratuberculosis in goat by Vineetha *et al.*, (2018), this pathosis was diagnosed as paucibacillary paratuberculosis. The characteristic histopathological lesions and morphology of granuloma cells of the present study is typical with description of Perez *et al.* (1996) and regarded as type III subtype *c* with characteristic multifocal granulomatous ileitis and paltry acid-fast bacilli.

Perivascular lymphocytic infiltration observed in this study was in agreement with Tafti and Rashidi (2000) and thought to be due to inflammatory reaction. Organised thrombus in the submucosa of ileum noticed in the present study was thought to be the MAP toxin induced endothelial damage with subsequent thrombus formation. This explains the toxin induced changes in other visceral organs as hepatitis, splenitis, nephritis and pneumonia.

Disseminated granulomatous lesions in lung, liver and kidney indicates the property of MAP to induce granulomatous lesions wherever it settles via circulation. Liver and lymph nodes are the most common secondary site of dissemination at the terminal stage of disease. The crux lesions of paratuberculosis such as lymph node fibrosis (Monika *et al.*, 2017), caseation with calcification (Sikandar *et al.*, 2013; Vineetha *et al.*, 2018) although absent, granulomatous pneumonia described in this study probably indicate the advanced clinical form of the disease as mentioned by previous workers (Copra, 2000).

MAP remains subclinical infections in ruminants and reverts to clinical disease especially due to stressors (Verma, 2013). Full term doe with twin foetuses probably contributed the stress factor for the development of clinical disease in the present goat.

## Conclusion

It was concluded from the above histopathological lesions in jejunum, ileum and MLNs that the case was diagnosed as multifocal type III subtype c paucibacillary paratuberculosis in a goat, which was confirmed by PCR.

## Conflict of Interests

There is no conflict of interest.

## Publisher Disclaimer

IJLR remains neutral concerning jurisdictional claims in published institutional affiliation.

## References

1. Bancroft, J.D. and Layton, C. (2019). The hematoxylin and eosin. In Suvarna SK, Layton C, Bancroft JD (Ed). Bancroft's theory and practice of histological techniques, 8<sup>th</sup> edition, Elsevier, 126-138.
2. Caspersen, O. (2003) Emaciated dairy cattle with poor welfare status are a growing problem. *Dansk Veterinaertidsskrift*, 86,12–14.
3. Catton, B.M. (2002). Paucibacillary paratuberculosis in a goat. *The Canadian Veterinary Journal*, 43,787-788.
4. Chiodini, R.J., Chamberlin, W.M., Sarosiek, J. and McCallum, R.W. (2012). Crohn's disease and the mycobacterioses: a quarter century later. Causation or simple association? *Critical Reviews in Microbiology*, 38(1),52-93.
5. Clarke, C.J. (1997). The pathology and pathogenesis of paratuberculosis in ruminants and other species. *Journal of Comparative Pathology*, 116,217-261.
6. Collins, D.M., Stephens, D.M. and de Lisle, G.W. (1993) Comparison of polymerase chain reaction tests and faecal culture for detecting *Mycobacterium paratuberculosis* in bovine faeces. *Veterinary Microbiology*, 36,289-299.
7. Copra, J.M., Garrido, J., Garcia-Marin, J.F. and Perez, V. (2000). Classification of lesions observed in natural cases of paratuberculosis in goats. *Journal of Comparative Pathology*, 122,255-265.
8. Dennis, M.M., Reddacliff, L.A., Whittington, R.J. (2011). Longitudinal study of clinicopathological features of Johne's disease in sheep naturally exposed to *Mycobacterium avium* subspecies paratuberculosis. *Veterinary Pathology*, 48(3),565-575.
9. Fiorentino, M.A., Gioffre, A., Cirone, K., Morsella, C., Alonso, B., Delgado, F. and Paolicchi, F. (2012). First isolation of *Mycobacterium avium* subsp. *paratuberculosis* in a dairy goat in Argentina: Pathology and molecular characterization. *Small Ruminant Research*, 108,133–136.
10. Garg, R., Patil, P.K., Singh, S.V., Sharma, S., Gandham, R.K., Singh, A.V., Filia, G., Singh, P.K., Jayaraman, S., Gupta, S., Chaubey, K.K., Tiwari, R., Saminathan, M., Dhama, K., Sohal, J.S. (2015). Comparative evaluation of different test combinations for diagnosis of *Mycobacterium avium* subspecies paratuberculosis infecting dairy herds in India. *BioMed Research International*, ID 983978,1-6.
11. Hailat, N.Q., Hananeh, W., Metekia, A.S., Stabel, J.R., Al-Majali, A. and Lafi, S. (2010). Pathology of subclinical paratuberculosis (Johne's Disease) in Awassi sheep with reference to its occurrence in Jordan. *Veterinari Medicina*, 55(12),590–602.
12. Johne, H.A. and Frothingham, L. (1895). Ein eigenthümlicher Fall von Tuberculose beim Rind Deut. *Zeits Tiermed Vergl Pathology*, 21,438-454.
13. Kirkwood, C.D., Wagner, J., Boniface, K., Vaughan, J., Michalski, W.P., Catto-Smith, A.G., Cameron, D.J. and Bishop R.F. (2009). *Mycobacterium avium* subspecies *paratuberculosis* in children with early onset Crohn's disease. *Inflammatory Bowel Diseases*, 15(11),1643–55.
14. Monika, T., Madhulina, M. and Gupta, V.K. (2017). Pathology of naturally occurring paratuberculosis in Gaddi goats of Himachal Pradesh. *Indian Journal of Veterinary Pathology*, 41(1),25-30.

15. Morris, G.B., Ridgway, E.J., Suvarna, S.K. (2019). Traditional stains and modern techniques for demonstrating microorganisms in histology. In Suvarna SK, Layton C, Bancroft JD (Ed). Bancroft's theory and practice of histological techniques, 8<sup>th</sup> edition, Elsevier, 260-261.
16. Perez, V., Garcia Martin, J.F. and Badiola, J.J. (1996). Description and classification of different types of lesion associated with natural paratuberculosis infection in sheep. *Journal of Comparative Pathology*, 2,107-122.
17. Rajkumar, K. and Tripathi, B.N. (2005). Histopathological spectrum and its relationship with humoral immune response in naturally occurring Caprine Paratuberculosis. *Indian Journal of Veterinary Pathology*, 29,71-77.
18. Sikandar, A., Cheema, A.H., Adil, M., Younus, M., Zaneb, H., Zaman, M.A., Tipu, M.Y. and Masood, S. (2013). Ovine paratuberculosis-a histopathological study from Pakistan. *Journal of Animal and Plant Sciences*, 23(3),749-753.
19. Sikandar, A., Cheema, A.H., Younus, M., Aslam, A., Zaman, M.A. and Rehman, T. (2012). Histopathological and serological studies on paratuberculosis in cattle and buffaloes. *Pakistan Veterinary Journal*, 32,547-557.
20. Singh, A., Yadav, M., Kumar, D., Sharma, P., Verma, A., Yadav, V. and Chauhan, D (2016). Prevalence and genotypes of *Mycobacterium avium* subspecies *paratuberculosis* in large ruminants of Eastern Uttar Pradesh, North India. *Journal of Advanced Laboratory Research in Biology*, 7(4),112-117.
21. Tafti, A.K. and Rashidi, K. (2000). The pathology of goat paratuberculosis: gross and histopathological lesions in the intestines and mesenteric lymph nodes. *Journal of Veterinary Medicine*, 47,487-495.
22. Twort, F.W. and Ingram, G.L.Y. (1913). A monograph of Johnes' disease. London: Barilliere, Tindall and Cox.
23. Verma, D.K. (2013). *Mycobacterium avium* subspecies *paratuberculosis*: an emerging animal pathogen of Global concern. *Advanced Biomedical Research*, 4,1-8.
24. Vineetha, S., Madhulina Maity., Singh, K.P., Sahoo, M., Saminathan, M., Chandan Prakash., Sardana, S., Sreelekshmy, M. and Singh, R. (2018). A case of hepato-renal syndrome associated with paratuberculosis in goat. *Indian Journal of Veterinary Pathology*, 42(2),122-126.
25. Whittington, R.J. and Sergeant, E.S. (2001) Progress towards understanding the spread, detection and control of *Mycobacterium avium* subsp. *Paratuberculosis* in animal population. *Australian Veterinary Journal*, 79(4),267-278.
26. Whittington, R.J., Begg, D.J., de Silva, K., Purdie, A.C., Dhand, N.K. and Plain, K.M. (2017). Case definition terminology for paratuberculosis. *BMC Veterinary Research*, 13,328.

\*\*\*\*\*